Pergamon

Int. J. Heat Mass Transfer. Vol. 40, No. 13, pp. 3069–3078, 1997

Printed in Great Britain
0017-9310/97 $17.00+0.00

PII: S0017-9310(96)00357-2

Natural convection along a wavy vertical plate to non-Newtonian fluids

E. KIM

School of Mechanical Engineering, Pusan National University, Pusan 609-735, South Korea

(*Received* 11 *June* 1996 *and in final form* 15 *October* 1996)

Abstract—A numerical investigation of natural convection flow along irregular vertical surfaces in non-Newtonian fluids is reported. A wavy vertical surface is used as an example to show the heat transfer mechanism near such surfaces. The results demonstrate that with an increase of flow index, the axial velocity increases, but the velocity boundary layer becomes thinner. The difference between the velocity in the crests and the troughs is indiscernible. The boundary layer around nodes is getting thicker compared to that of the crests and the troughs. When the natural convection boundary layer grows thick, the amplitude of the local Nusselt number gradually decreases. The effects of Prandtl number, flow index and surface amplitude in non-Newtonian fluids are also discussed in detail. © 1997 Elsevier Science Ltd.

1. INTRODUCTION

The classical problem of laminar natural convection heat transfer in a Newtonian fluid along a vertical plate is well known. In general, it is not vertical surfaces or Newtonian fluids for many practical applications. The objective of this work is to analyze the natural convection heat transfer of non-Newtonian fluids along a wavy vertical plate. For Newtonian fluids, Sparrow *et al.* [1] developed the similarity solution for the non-isothermal boundary condition on a vertical plate. Several researchers [2–5] have studied vertical systems under various boundary conditions. Recently, Yao [6–8] studied the effects of a wavy surface on thermal bodies. Proposing that the surfaces of the fluid flow are not uniform, but irregular surfaces in practical situations, he used a simple coordinate transformation method to change the wavy surface into a flat surface. In 1995, Rees and Pop [9] investigated the effects of nonuniformities on a large-scale surface in a porous medium. In this research, they assumed that when the Rayleigh number is high, the amplitude of a wave has a close order with a wavelength. In their results, the highest thermal point occurred when the slope of a surface geometry function was a maximum. All these [6–9] were done in Newtonian fluids. In general, non-Newtonian fluids are more practical and applicable to many technological areas. A review of developments to 1982 was presented by Shenoy and Mashelkar [10]. Recent contributions in the area of natural convection of non-Newtonian fluids along vertical surfaces were made by [11–13] theoretically and [14] experimentally, respectively.

All previous theoretical and experimental studies, however, considered only flat plates or simple two-dimensional bodies. So, it is necessary to study the heat transfer mechanism on non-Newtonian fluids with a complex geometry which is easily encountered in heat transfer enhancement devices such as cooling fins. In this paper the effects of a wavy surface, temperature profiles, Prandtl number and flow index for non-Newtonian fluids are investigated.

2. MATHEMATICAL ANALYSIS AND NUMERICAL METHOD

A physical geometry and coordinate system of a wavy vertical plate is shown in Fig. 1. The surface of the vertical plate is described by $y = \sigma(x)$ where $\sigma(x)$ is an arbitrary geometry function. The profile of the surface shown in Fig. 1 is

$$y = \sigma(x) = \alpha \sin(2\pi x). \tag{1}$$

Here, α is the non-dimensional amplitude of the wavy surface. The ambient temperature is maintained at a constant temperature T_∞ and the surface of the plate is kept at a constant temperature T_w. The flow is steady and two-dimensional. All fluid properties are constant except the density in the buoyancy force term, and it is assumed that the Boussinesq approximation is valid. The Cauchy stress for power-law fluids can be written as,

$$\mathbf{T} = -P\mathbf{I} - m|\sqrt{(\tfrac{1}{2}\mathbf{A}_1\mathbf{A}_2)}|^{n-1}\mathbf{A}_1. \tag{2}$$

Here P is the pressure, $\mathbf{I}$ is the Kronecker delta, m is the consistency index, n is the power-law flow index, $\mathbf{A}_1$ and $\mathbf{A}_2$ are, respectively, the first Rivlin–Ericksen tensor and the second Rivlin–Ericksen tensor.

NOMENCLATURE

a	amplitude of wave
$\mathbf{A}_1$	first Rivlin–Ericksen tensor
$\mathbf{A}_2$	second Rivlin–Ericksen tensor
c_p	specific heat
g	gravitational acceleration
h_x	local heat transfer coefficient
$\mathbf{I}$	Kronecker delta
k	thermal conductivity of fluid
l	wavelength
m	consistency index
n	power-law index
N_{gr}	generalized Grashof number
N_{pr}	generalized Prandtl number
Nu_x	local Nusselt number
P	pressure
q	heat flux
T	temperature
u, v	velocity components in (x, y) directions
x, y	coordinates.

Greek symbols

α	dimensionless amplitude of wave
β	thermal expansion coefficient
θ	dimensionless temperature
ρ	density
σ	surface geometry function.

Superscripts

$\bar{}$	dimensionless quantity
$\hat{}$	dimensionless quantity
$'$	derivative with respect to x.

Subscripts

w	wall
∞	free stream.

The conservation equations for steady laminar flow can be written as

$$\nabla \cdot \mathbf{T} + \rho \mathbf{b} = \rho \frac{\mathrm{d}\mathbf{v}}{\mathrm{d}t} \tag{3}$$

$$\nabla \cdot \mathbf{v} = 0 \tag{4}$$

$$\rho c_p \mathbf{v} \cdot \nabla = k \nabla^2 T. \tag{5}$$

Here $\mathbf{v}$ is the velocity vector, T temperature, c_p specific heat, k thermal conductivity. The body force, $\mathbf{b}$, for the natural convection situation can be defined as

$$\mathbf{b} = \beta g (T - T_\infty) \hat{j}. \tag{6}$$

The governing equations (equations (3)–(5)) are transformed from a physical coordinate system (x, y) to a dimensionless coordinate system $(\bar{x}, \bar{y})$ by using the following transformation and dimensionless quantities:

$$\bar{x} = \frac{x}{l} \quad \bar{y} = \frac{y - \sigma(x)}{l} N_{gr}^{1/(2(n+1))} \tag{7}$$

$$\bar{u} = \frac{u}{\sqrt{lg\beta\Delta T}} \quad \bar{v} = \frac{v - \sigma' u}{\sqrt{lg\beta\Delta T}} N_{gr}^{1/(2(n+1))} \tag{8}$$

$$\Theta = \frac{T - T_\infty}{T_w - T_\infty} \tag{9}$$

$$\bar{P} = \frac{P}{\rho l g \beta \Delta T} \tag{10}$$

$$\sigma' = \frac{\mathrm{d}\sigma}{\mathrm{d}x} = \frac{\mathrm{d}\bar{\sigma}}{\mathrm{d}\bar{x}} \tag{11}$$

$$N_{gr} = \frac{\rho^2 l^{n+2} [\beta g \Delta T]^{2-n}}{m^2} \tag{12}$$

$$N_{pr} = \frac{\rho c_p}{k} \left(\frac{m}{\rho}\right)^{2/(1+n)} (l)^{(1-n)/(1+n)} [l\beta g \Delta T]^{(3(1-n))/(2(1+n))} \tag{13}$$

where N_{gr} and N_{pr} are the generalized Grashof number and the generalized Prandtl number, respectively.

By using the coordinate transformation equation (7), the boundary surface can be transformed from the wavy vertical surface to a flat surface. Under the assumption of a large Grashof number, the conservation equations of mass, linear momentum, and energy, equations (3)–(5), can be written as

$$\frac{\partial \bar{u}}{\partial \bar{x}} + \frac{\partial \bar{v}}{\partial \bar{y}} = 0 \tag{14}$$

$$\bar{u}\frac{\partial \bar{u}}{\partial \bar{x}} + \bar{v}\frac{\partial \bar{u}}{\partial \bar{y}} = -\frac{\partial \bar{P}}{\partial \bar{x}} + \sigma' N_{gr}^{1/(2(n+1))} \frac{\partial \bar{P}}{\partial \bar{y}} + \Theta + (1 + \sigma'^2)^n \frac{\partial}{\partial \bar{y}} \left(\frac{\partial \bar{u}}{\partial \bar{y}}\right)^n \tag{15}$$

$$\sigma'^2 \bar{u}^2 + \sigma' \Theta = \sigma' \frac{\partial \bar{P}}{\partial \bar{x}} - (1 + \sigma'^2) N_{gr}^{1/(2(n+1))} \frac{\partial \bar{P}}{\partial \bar{y}} \tag{16}$$

$$\bar{u}\frac{\partial \Theta}{\partial \bar{x}} + \bar{v}\frac{\partial \Theta}{\partial \bar{y}} = -\frac{1}{N_{pr}}(1 + \sigma'^2)\frac{\partial^2 \Theta}{\partial \bar{y}^2}. \tag{17}$$

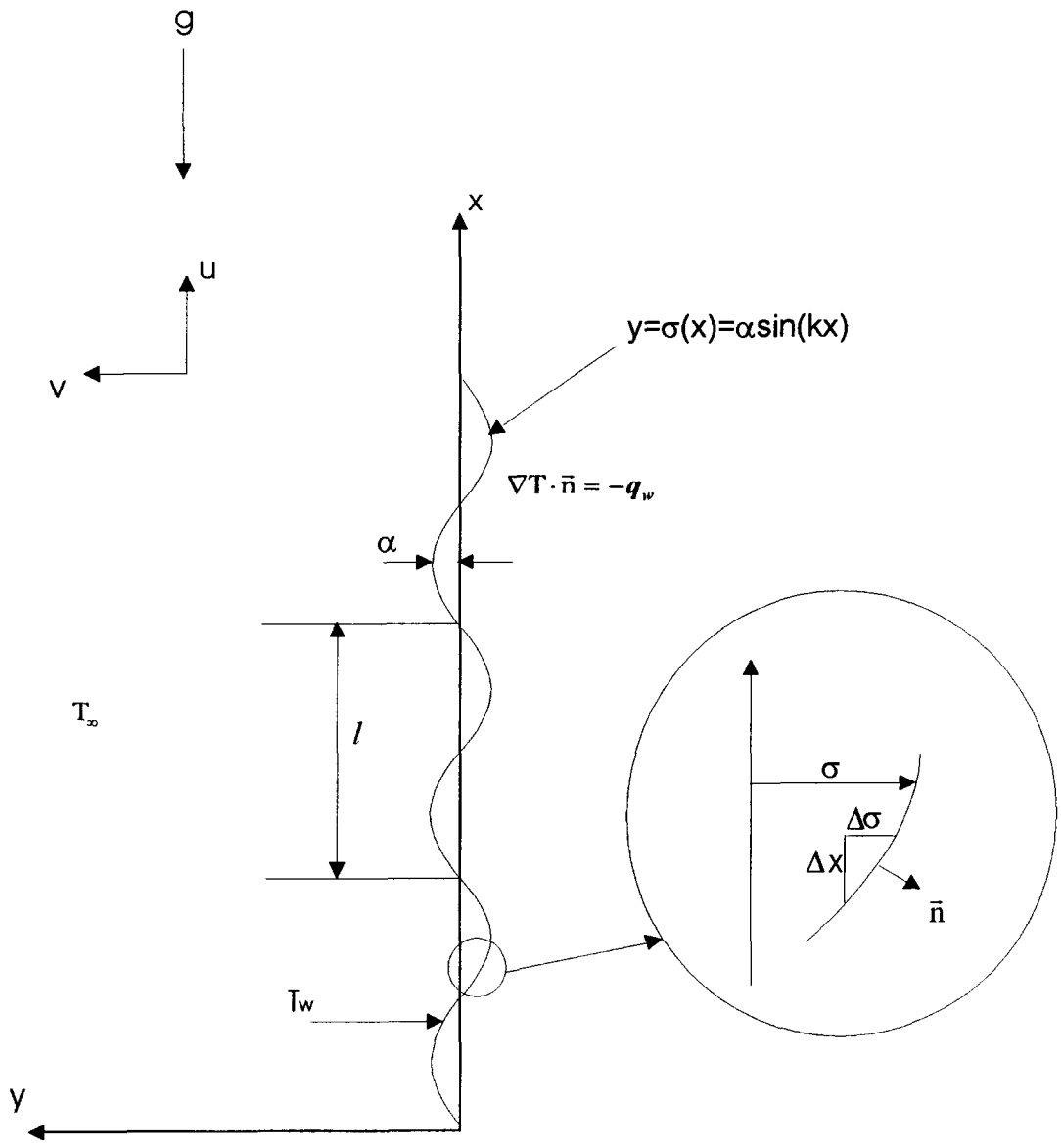

Fig. 1. Physical model and coordinate system.

It is noted, from equation (16), that the pressure gradient along the $\bar{y}$-direction is $O(N_{gr}^{(-1/2(n+1))})$ and is determined by the left-hand side of the equation. The pressure gradient in the $\bar{x}$-direction can, then, be obtained from the potential flow theory. In the current problem, $\partial\bar{P}/\partial\bar{y} = 0$. Elimination of $\partial\bar{P}/\partial\bar{y} = 0$ in equations (15) and (16) yields three equations in $\hat{u}$, $\hat{v}$ and Θ in a parabolic coordinate $(\hat{x}, \hat{y})$:

$$\hat{x} = \bar{x} \tag{18}$$

$$\hat{y} = \frac{\bar{y}}{[2(n+1)\bar{x}]^{1/(2(n+1))}} \tag{19}$$

$$\hat{u} = \frac{\bar{u}}{[2(n+1)\bar{x}]^{1/2n}} \tag{20}$$

$$\hat{v} = [2(n+1)\bar{x}]^{1/(2(n+1))}\bar{v}. \tag{21}$$

(1) conservation of mass

$$\frac{n+1}{n}\hat{u} + [2(n+1)\hat{x}]\frac{\partial\hat{u}}{\partial\hat{x}} - \hat{y}[2(n+1)\hat{x}]^{((n-1)(2n+1))/(2n(n+1))}\frac{\partial\hat{v}}{\partial\hat{y}} = 0. \tag{22}$$

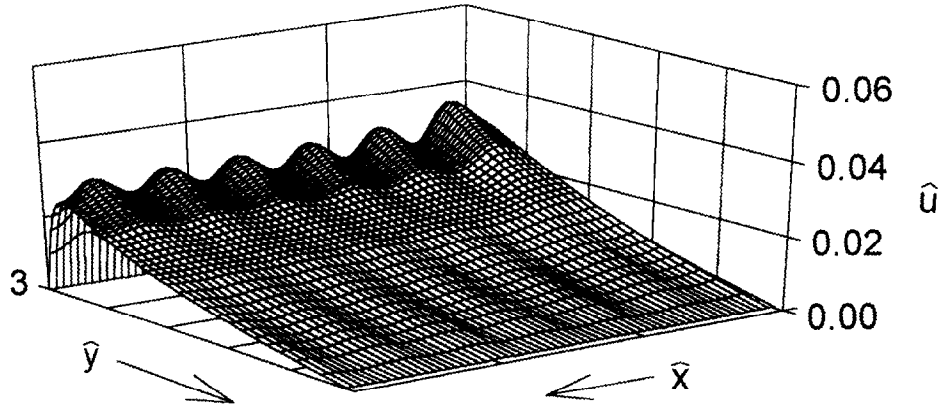

(a) n=0.8

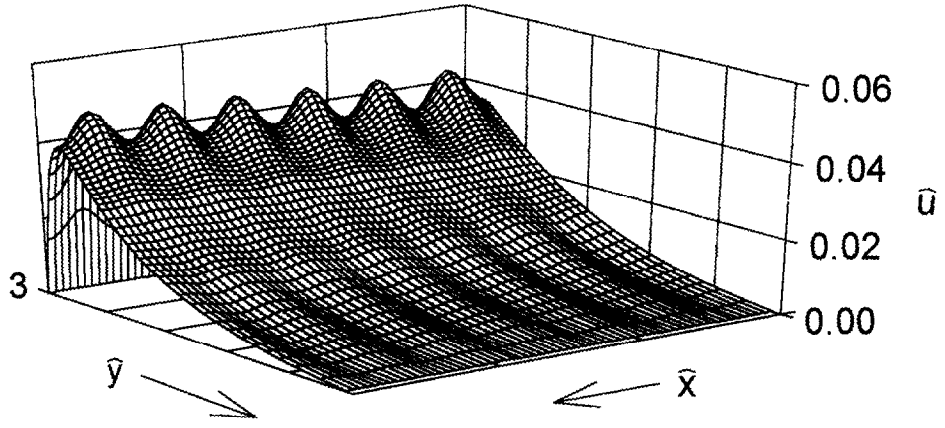

(b) n=1.0

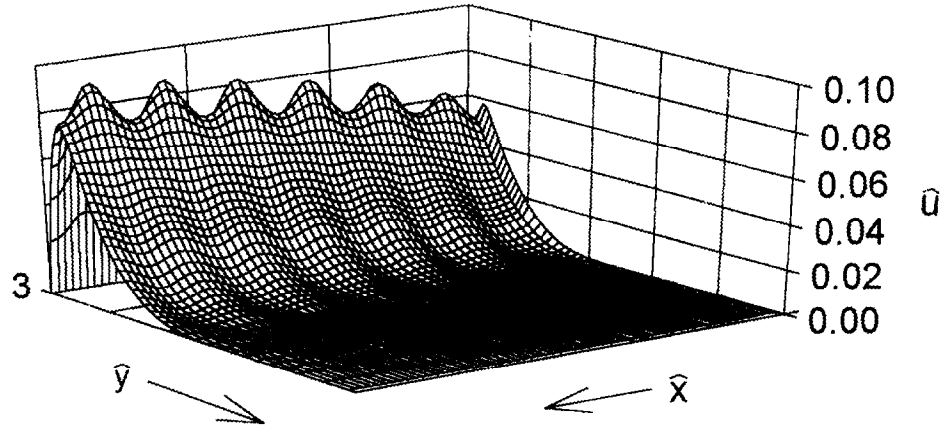

(c) n=1.2

Fig. 2. Axial velocity distribution for $\alpha = 0.1$.

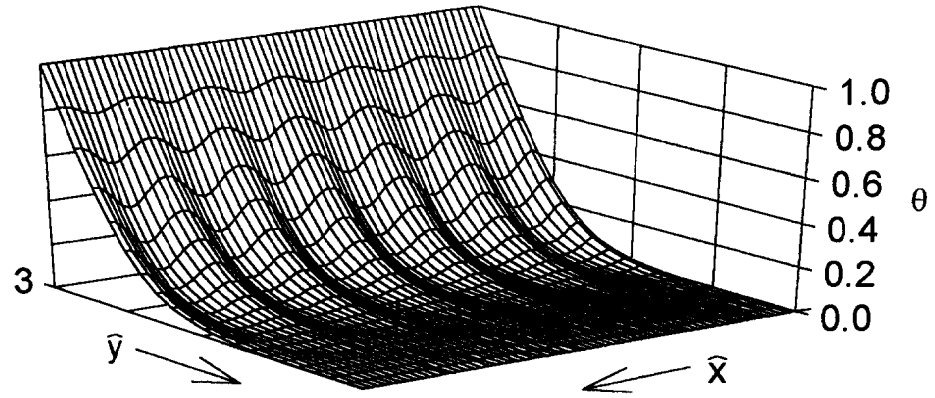

(a) n=0.8

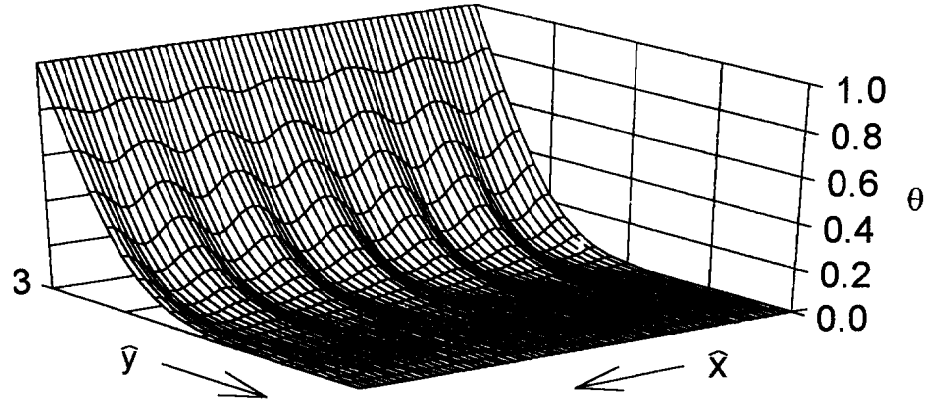

(b) n=1.0

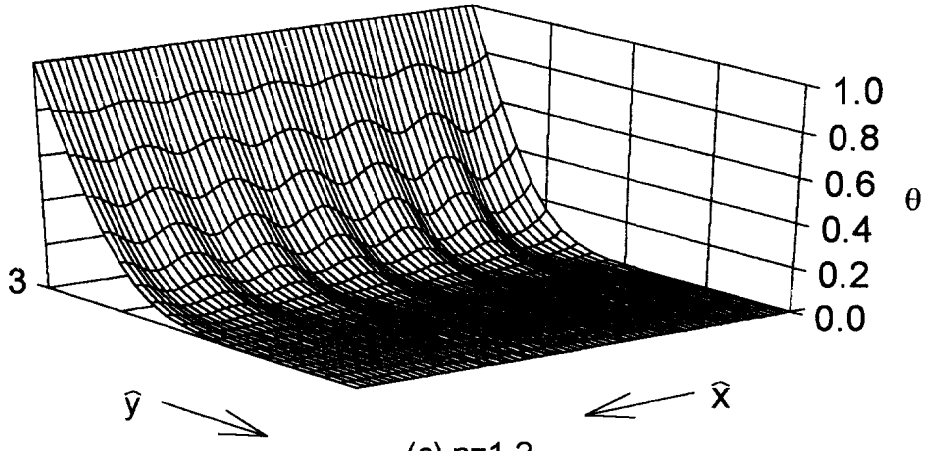

(c) n=1.2

Fig. 3. Dimensionless temperature distribution for $\alpha = 0.1$.

(2) conservation of linear momentum

$$[2(n+1)\hat{x}]^{1/n}\hat{u}\frac{\partial\hat{u}}{\partial\hat{x}}+([2(n+1)\hat{x}]^{(1-n)/(2n(n+1))}-[2(n+1)\hat{x}]^{(1-n)/n}\hat{y}\hat{u})\frac{\partial\hat{u}}{\partial\hat{y}}$$
$$=-\left(\frac{n+1}{n}[2(n+1)\hat{x}]^{(1-n)/n}+\frac{\sigma'\sigma''[2(n+1)\hat{x}]^{1/n}}{1+\sigma'^2}\right)\hat{u}^2+\frac{\Theta}{1+\sigma'^2}+(1+\sigma'^2)^n\frac{\partial}{\partial\hat{y}}\left(\frac{\partial\hat{u}}{\partial\hat{y}}\right)^n. \quad (23)$$

(3) conservation of energy

$$[2(n+1)\hat{x}]^{(3n+1)/[2n(n+1)]}\hat{u}\frac{\partial\Theta}{\partial\hat{x}}+(\hat{v}-[2(n+1)\hat{x}]^{((1-n)(1+2n))/(2n(1+n))}\hat{y}\hat{u})\frac{\partial\Theta}{\partial\hat{y}}$$
$$=-\frac{1}{N_{\rm pr}}(1+\sigma'^2)\frac{\partial^2\Theta}{\partial\hat{y}^2}. \quad (24)$$

The appropriate transformed boundary conditions are:

$$\hat{u}=\hat{v}=0 \quad \text{at } \hat{y}=0 \quad (25)$$

$$\Theta=1 \quad (26)$$

$$\hat{u}\to 0 \quad \text{as } \hat{y}\to\infty \quad (27)$$

$$\Theta=0. \quad (28)$$

The dimensionless governing equations (22)–(24) and the boundary conditions (25)–(28) are solved by the finite volume method which is discussed by Patankar [15]. The numerical grids in a computation domain are easy to fit a rectangular coordinate system. Mapping a curvilinear coordinate to the rectangular coordinate reduces the effort of numerical calculation. The discretized governing equations were solved by a line-by-line technique, which utilizes a tri-diagonal-matrix algorithm for the solution along each line of unknowns.

3. RESULTS AND DISCUSSION

To obtain results with high accuracy, the nodes must be very fine near the wall and can gradually turn to a coarser grid in the $\hat{y}$-direction. Numerical results were calculated with $\sigma=\alpha\sin(2\pi x)$ to show the

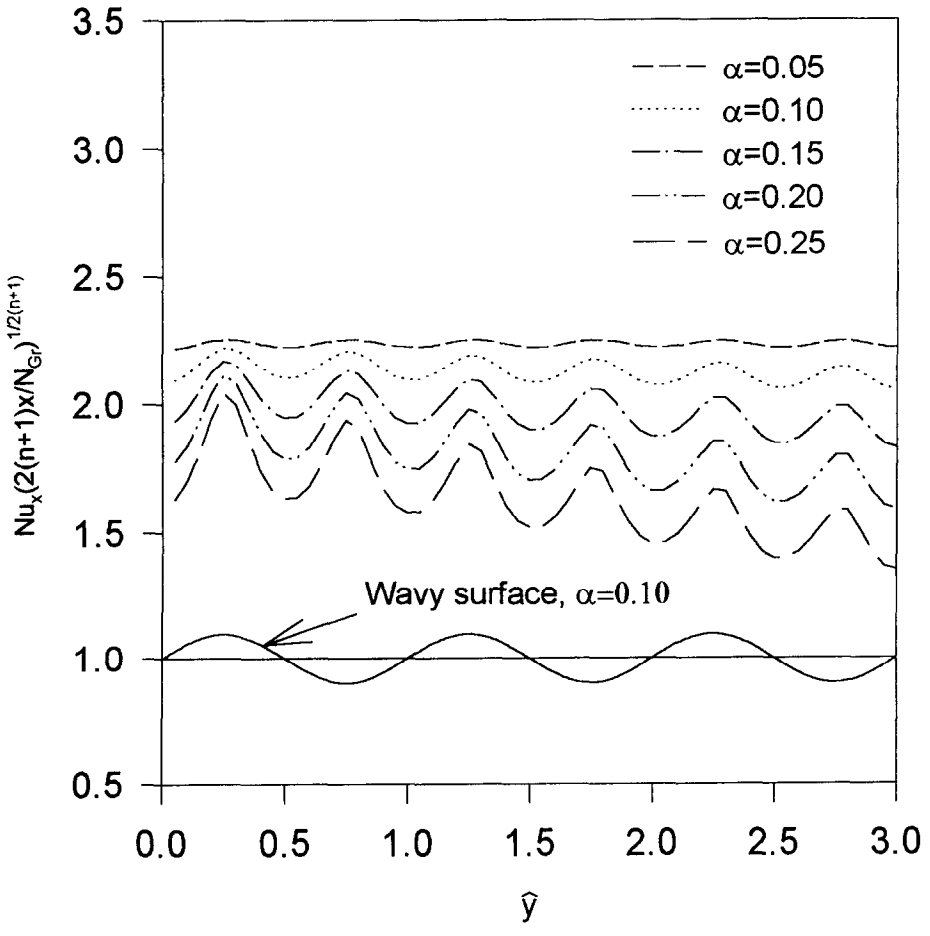

Fig. 4. Comparison of local heat transfer rate for $n=0.1$.

advantages of the transformation method and effect of the wavy surface in natural convection. For a different geometry the appropriate function σ can be used. With a small curvilinear surface, for example $\sigma \approx O(N_{gr}^{-1/2(n+1)})$, the effect of the wave surface is negligible and the governing equations can be assumed to be those for the flat plate. However, for a uniform amplitude surface, the curvature effects are important, and can not be neglected. To validate the numerical accuracy of the solution procedure, the numerical results of velocities, temperature and heat transfer coefficient for the case of Newtonian fluids over a wavy vertical plate were compared with those of Yao [6]. The results agreed within 1%. Further details are given by Kim and Chen [16].

The governing equations for natural convection with a non-Newtonian fluid have been numerically solved for three different flow indices, $n = 0.8$, 1.0 and 1.2. They represent pseudoplastic fluids, Newtonian fluids, dilatant fluids, respectively. The velocity profiles of the dimensionless amplitude $\alpha = 0.1$ ($\alpha = a/l$ is the dimensionless wave amplitude of the wavy plate) were shown in Fig. 2(a–c). It can be seen from these figures that the maximum $\hat{x}$-components of the velocity increase but the velocity boundary layer becomes thinner with the increase of flow index. Figure 3(a–c) shows the dimensionless temperature profiles for each case of n values. The thermal boundary layers of pseudoplastic fluids are thinner than those of dilatant fluids. The temperature gradient taken from Fig. 3(a–c) must consider the effects of local curvature, because the $\hat{y}$-direction is not vertical to the wavy surface. The local heat transfer coefficient, which is defined by Newton's law of cooling, may be determined by using the heat balance at the boundary. In accordance with Fourier's law the absolute value of the heat flux (see Fig. 1) is

$$q(x) = -k\vec{n} \cdot \nabla T \tag{29}$$

where

$$n_x = -\frac{\sigma'}{\sqrt{1+\sigma'^2}}, \quad n_y = \frac{1}{\sqrt{1+\sigma'^2}}.$$

Using Newton's law of cooling and Fourier's law in equation (29), the resulting equation is

$$Nu_x \left(\frac{2(n+1)\hat{x}}{N_{gr}}\right)^{1/(2(n+1))} = -(1+\sigma'^2)^{1/2} \frac{\partial \Theta}{\partial \hat{y}}\bigg|_{\hat{y}=0}. \tag{30}$$

Figure 4 shows the profiles of the Nusselt number obtained by using equation (30) for the case of dimensionless amplitude $\alpha = 0.05$, 0.10, 0.15, 0.20 and 0.25. The local heat transfer rate for the wavy vertical plate decreases when α increases. For the vertical plate the buoyancy force is parallel to the velocity profile. However, the buoyancy force of the irregular surface is smaller than that of the vertical plate except at the highest and the lowest points. The wavelength of the local Nusselt number is half of that of the wavy surface. As the dimensionless amplitudes increase, the effects of geometry are more pronounced. However, the effects of amplitude gradually decrease as the natural convection boundary layers grow thicker along the plate.

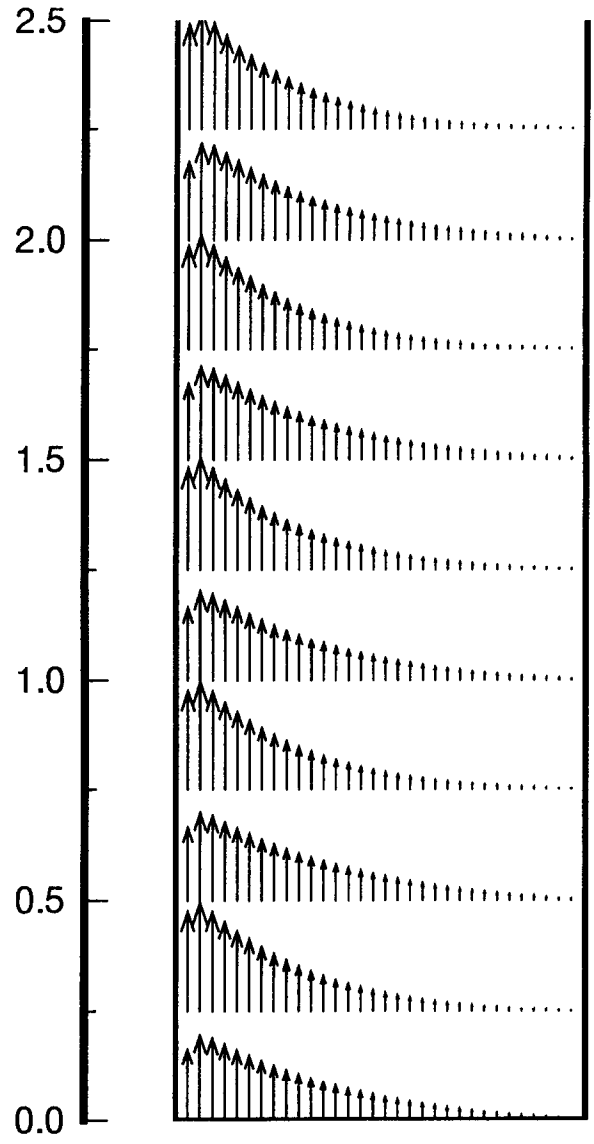

Fig. 5. Axial velocity profile.

Figure 5 shows the dimensionless axial velocity profiles past the wavy vertical surface for the case of $\alpha = 0.1$. The axial velocity profiles are sinusoidal along $\hat{x}$-direction. The regular nodes along the $\hat{x}$-direction are $\hat{x} = 1.5$, 2.0. $\hat{x} = 1.75$ and $\hat{x} = 2.25$ represent the trough and the crest of one wavy segment, respectively. The difference in the velocity in the crest and the trough is indiscernible. The boundary layer around the nodes is thicker compared to that of the crests or the troughs. It must be emphasized that the velocity component along the $\hat{x}$-direction in the computation domain is not paralleled to the physical

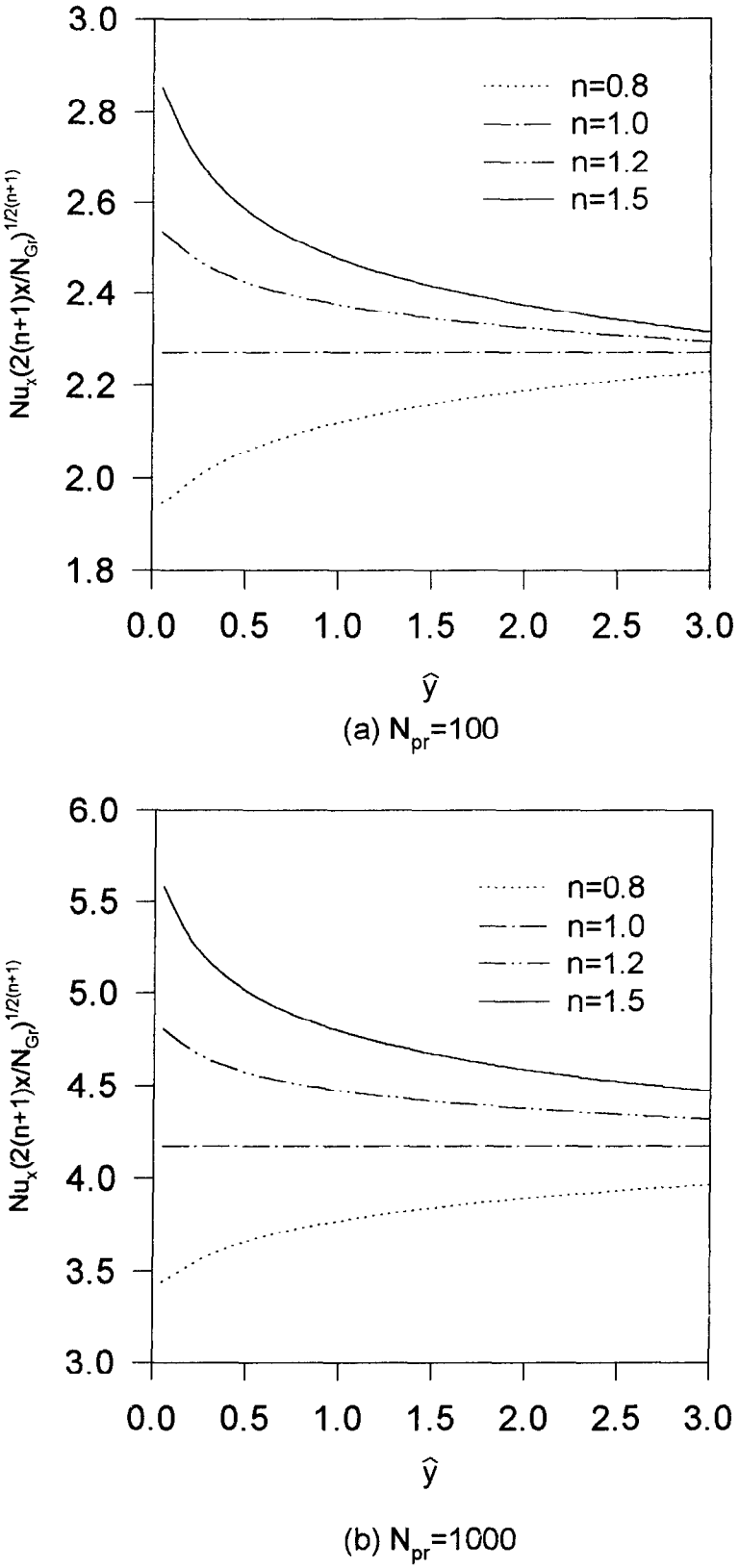

Fig. 6. Local Nusselt number for $\alpha = 0.0$.

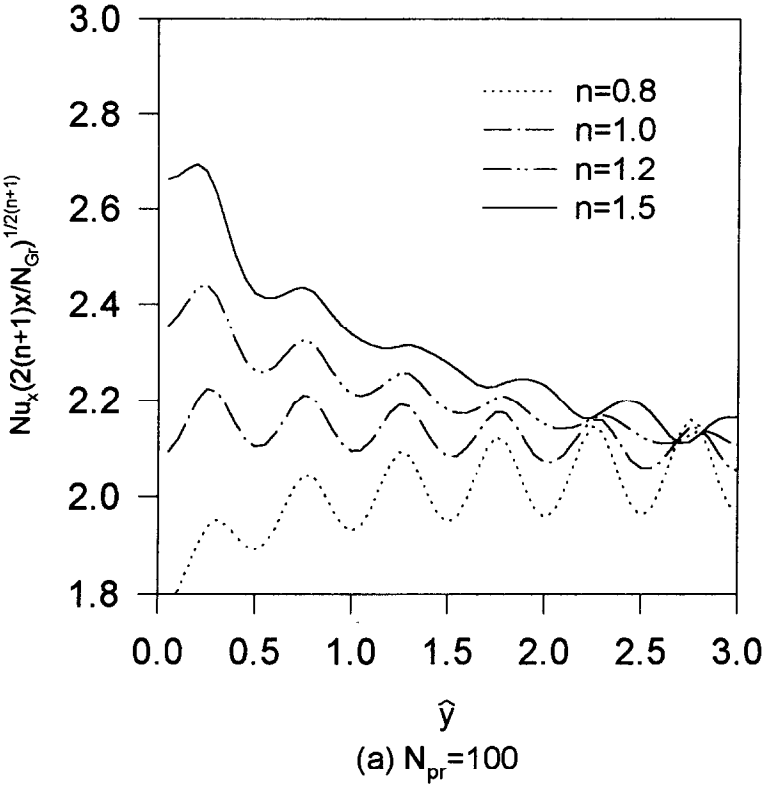

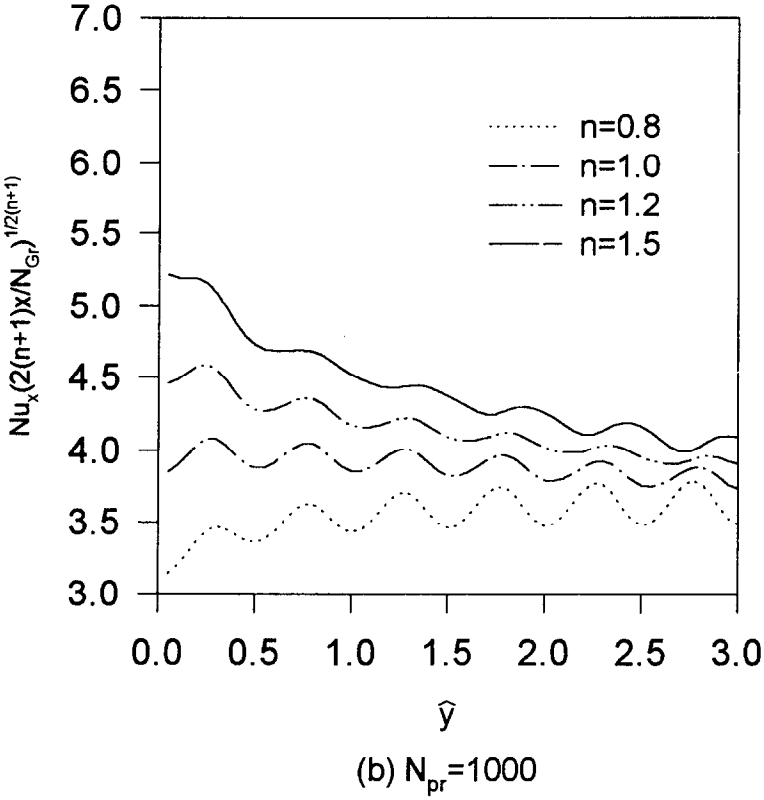

Fig. 7. Local Nusselt number for $\alpha = 0.1$.

surface. The local heat transfer rate cannot be obtained from the velocity component of the $\hat{x}$-direction.

Figures 6 and 7 show the variation of the local heat transfer rate as a function of Prandtl number, Pr and the flow index n for the cases of $\alpha = 0.0, 0.1$. As can be seen from the figures, the local heat transfer rate along the axial direction increases for dilatant fluids while decreases for pseudoplastic fluids. With the increase of the Prandtl number, the local heat transfer rate is getting higher except around the leading edge of the surface. Distributions of the local Nusselt number are illustrated in Fig. 7 for $\alpha = 0.1$. From the figure, the curves asymptotically approach a constant. The wavelength of the local heat transfer rate corresponds to half of that of the wavy surface. The variation of heat transfer rate decreases for dilatant fluid and this shows the natural convection buoyancy layer is getting thicker along the $\hat{x}$-direction. The curvilinear effects of the surface for the viscous boundary layer correspond to the diffusion process. These effects are getting smaller when the boundary layer is fully developed.

4. CONCLUSIONS

Solutions of the effects of a irregular geometry in non-Newtonian fluids were investigated. Non-dimensional analyses were applied with the assumption that the Grashof number is large for the natural convection boundary layer. To show the effects of non-Newtonian fluids, the parameters like flow index, Prandtl number and Nusselt number were considered. For the thermal heat transfer coefficients, the effect of the geometry is large at the starting point of the vertical surface, however it decreases with increasing $\hat{x}$. The thermal boundary layer of pseudoplastic fluids is thinner than that of dilatant fluids. The wavelength of the local Nusselt number is half that of the wavy surface and the effects of amplitude decrease in the downstream direction. When the dimensionless amplitude α increases, the amplitude of the surface increases and the local Nusselt number decreases. For a more profound understanding, experimental data are needed to examine the physical mechanism near irregular surfaces.

Acknowledgements—The author would like to express sincere appreciation to Dr J. L. S. Chen for valuable comment on the interpretation of the results.

REFERENCES

1. Sparrow, E. M. and Gregg, J. L., Similar solutions for free convection from a nonisothermal vertical plate. *Transactions of the ASME*, 1957, **79,** 379–385.
2. Brodowicz, K., On analysis of laminar free convection around isothermal vertical plate. *International Journal of Heat and Mass Transfer*, 1968, **11,** 201–209.
3. Hieber, C. A., Natural convection around a semi-infinite vertical plate. *International Journal of Heat and Mass Transfer*, 1974, **17,** 785–791.
4. Churchill, S. W. and Chu, H. H. S., Correlation equations for laminar and turbulent free convection from a vertical plate. *International Journal of Heat and Mass Transfer*, 1975, **18,** 1323–1329.
5. Kawase, Y. and Ulbrecht, J. J., Approximate solution to the natural convection heat transfer from a vertical plate. *International Communication of Heat and Mass Transfer*, 1984, **11,** 143–155.
6. Yao, L. S., Natural convection along a vertical wavy surface. *Journal of Heat Transfer*, 1983, **105,** 465–468.
7. Moulic, S. G. and Yao, L. S., Mixed convection along a wavy surface. *Journal of Heat Transfer*, 1989, **111,** 974–979.
8. Yao, L. S., A note on Prandtl's transposition theorem. *Journal of Heat Transfer*, 1988, **110,** 507–508.
9. Rees, D. A. S. and Pop, I., Free convection induced by a vertical wavy surface with uniform heat flux in a porous medium. *Journal of Heat Transfer*, 1995, **117,** 547–550.
10. Shenoy, A. V. and Mashelkar, R. A., Thermal convection in non-Newtonian fluids. *Advances in Heat Transfer*, 1982, **15,** 143–225.
11. Som, A. and Chen, J. L. S., Free convection of non-isothermal two-dimensional bodies. *International Journal of Heat and Mass Transfer*, 1984, **27,** 791–794.
12. Kleinstreuer, C., Wang, T. Y. and Haq, S., Natural convection heat transfer between a power-law fluid and a permeable isothermal vertical wall. *ASME Publication HTD*, 1987, **97,** 25–31.
13. Huang, M., Huang, J., Chou, Y. and Chen, Y., Effects of Prandtl number on free convection heat transfer from a vertical plate to a non-Newtonian fluid. *Journal of Heat Transfer*, 1989, **111,** 189–191.
14. Dale, J. D. and Emery, A. F., The free convection of heat from a vertical plate to several non-Newtonian "pseudoplastic" fluids. *Journal of Heat Transfer*, 1972, **94,** 64–72.
15. Patanker, S. V., *Numerical Heat Transfer and Fluid Flow*. Hemisphere, Washington, 1980.
16. Kim, E. and Chen, J. L. S., Natural convection of non-Newtonian fluids along a wavy vertical plate. *The 28th National Heat Transfer Conference (ASME)*, Minnesota, 1991, pp. 45–49.